

CBGL: Fast Monte Carlo Passive Global Localisation for 2D LIDAR Sensors

Alexandros Filotheou

Abstract—Lorem ipsum dolor sit amet, consectetur adipiscing elit. Ut purus elit, vestibulum ut, placerat ac, adipiscing vitae, felis. Curabitur dictum gravida mauris. Nam arcu libero, nonummy eget, consectetur id, vulputate a, magna. Donec vehicula augue eu neque. Pellentesque habitant morbi tristique senectus et netus et malesuada fames ac turpis egestas. Mauris ut leo. Cras viverra metus rhoncus sem. Nulla et lectus vestibulum urna fringilla ultrices. Phasellus eu tellus sit amet tortor gravida placerat. Integer sapien est, iaculis in, pretium quis, viverra ac, nunc. Praesent eget sem vel leo ultrices bibendum. Aenean faucibus. Morbi dolor nulla, malesuada eu, pulvinar at, mollis ac, nulla. Curabitur auctor semper nulla. Donec varius orci eget risus. Duis nibh mi, congue eu, accumsan eleifend, sagittis quis, diam. Duis eget orci sit amet orci dignissim rutrum.

CBGL leverages the relationships of (a) proportionality between the pose estimate error and the value of the Cumulative Absolute Error per Ray (CAER) metric for pose estimates in a neighbourhood of the sensor's pose, and (b) lack of disproportionality outside of that neighbourhood

Index Terms—global localisation, 2D LIDAR, monte carlo, scan-to-map-scan matching

I. INTRODUCTION

This paper addresses the problem of Passive Global Localisation of a 2D LIDAR sensor, i.e. the estimation of its location and orientation within a given map, under complete locational and orientational uncertainty, without prescribing motion commands (to the mobile robot that the sensor is assumed mounted to) for further knowledge acquisition. Specifically the problem is formalised in Problem P:

Problem P. Let the unknown pose of an immobile 2D range sensor whose angular range is λ be $\mathbf{p}(\mathbf{l}, \theta)$, $\mathbf{l} = (x, y)$, with respect to the reference frame of map M . Let the range sensor measure range scan \mathcal{S}_R . The objective is the estimation of \mathbf{p} given M , λ , and \mathcal{S}_R .

II. DEFINITIONS

Let $\mathcal{A} = \{\alpha_i : \alpha_i \in \mathbb{R}\}$, $i \in \mathbb{I} = \langle 0, 1, \dots, n-1 \rangle$, denote a set of n elements, $\langle \cdot \rangle$ denote an ordered set, \mathcal{A}_{\uparrow} the set \mathcal{A} ordered in ascending order, the bracket notation $\mathcal{A}[\mathbb{I}] = \mathcal{A}$ denote indexing, and notation $\mathcal{A}_{k:l}$, $0 \leq k \leq l$, denote limited indexing: $\mathcal{A}_{k:l} = \{\mathcal{A}[k], \mathcal{A}[k+1], \dots, \mathcal{A}[l]\}$.

Definition I. *Range scan captured from a 2D LIDAR sensor.*—A conventional 2D LIDAR sensor provides a finite number of ranges, i.e. distances to objects within its range, on a horizontal cross-section of its environment, at regular angular and temporal intervals, over a defined angular range [1]. A range scan \mathcal{S} , consisting of N_s rays over an angular range λ , is an ordered map $\mathcal{S} : \Theta \rightarrow \mathbb{R}_{\geq 0}$, $\Theta = \{\theta_n \in [-\frac{\lambda}{2}, +\frac{\lambda}{2}] : \theta_n = -\frac{\lambda}{2} + \lambda \frac{n}{N_s}, n = 0, 1, \dots, N_s-1\}$. Angles

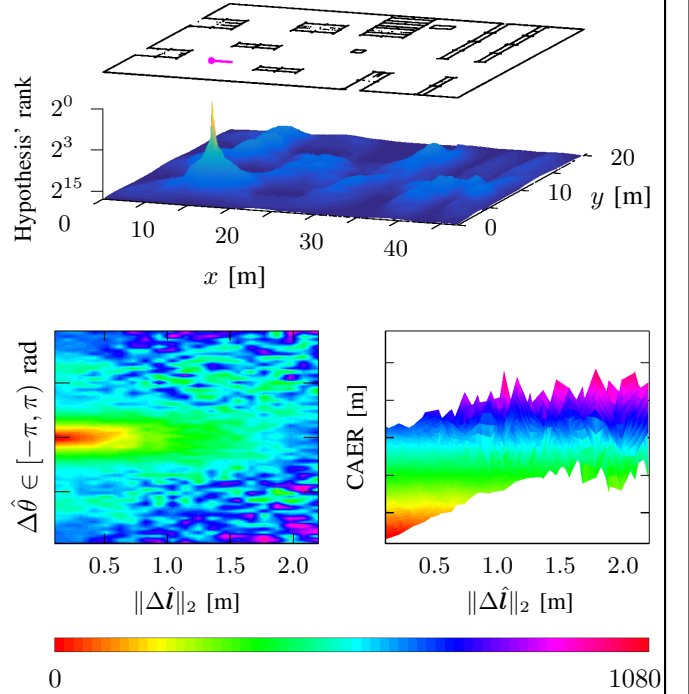


Fig. 1: Given a LIDAR sensor's 2D measurement, at its core, CBGL disperses pose hypotheses within the map and ranks them ascendingly according to the value of the CAER metric. This produces a $\mathbf{r}(\text{rank})$ -field which may be used to estimate the pose of the sensor (a) accurately due to the proportionality of estimate error and CAER, and (b) quickly due to the metric's low computational complexity. Top: a map of an environment, the pose of a panoramic 2D LIDAR sensor (magenta), and the corresponding CAER rank field below them. Bottom: distribution of CAER values by location and orientation error of all sensor pose hypotheses corresponding to the rank field above, for estimate distances up to 2.0 m. In this example the map's area is 735 m², and 10⁶ hypotheses are dispersed randomly in its free space for 100 trials; CBGL's maximum location error and maximum execution time is, respectively, 0.062 m and 8.8 sec

θ_n are expressed relative to the sensor's heading, in the sensor's frame of reference.

Definition II. *Map-scan.*—A map-scan is a virtual scan that encapsulates the same pieces of information as a scan derived from a physical sensor. Only their underlying operating principle is different due to the fact the map-scan refers to distances to the boundaries of a point-set, referred to as the map, rather than within a real environment. A map-scan $\mathcal{S}_V^M(\hat{\mathbf{p}})$ is derived by means of locating intersections of rays emanating from the estimate of the sensor's pose estimate $\hat{\mathbf{p}}$ and the boundaries of the map M .

Definition III. CAER as metric.—Let \mathcal{S}_p and \mathcal{S}_q be two range scans, equal in angular range λ and size N_s . The value of the Cumulative Absolute Error per Ray (CAER) metric $\psi \in \mathbb{R}_{\geq 0}$ between \mathcal{S}_p and \mathcal{S}_q is given by

$$\psi(\mathcal{S}_p, \mathcal{S}_q) \triangleq \sum_{n=0}^{N_s-1} |\mathcal{S}_p[n] - \mathcal{S}_q[n]| \quad (1)$$

Definition IV. CAER as field.—A ψ -field on map M $f_\psi^M : \mathbb{R}^2 \times [-\pi, +\pi) \rightarrow \mathbb{R}_{\geq 0}$ is a mapping of 3D pose configurations $\hat{p}(\hat{x}, \hat{y}, \hat{\theta})$ to CAER values (def. III) such that if $\psi(\mathcal{S}_R, \mathcal{S}_V^M(\hat{p})) = c$ then $f_\psi^M(\hat{p}) = c$. In other words a CAER field is produced by computing the value of the CAER metric between a range scan \mathcal{S}_R (def. I) and a map-scan $\mathcal{S}_V^M(\hat{p})$ captured from pose configuration \hat{p} within map M (def. II).

Definition V. Rank field.—Let f_ψ^M be a ψ -field on map M and $\mathcal{P} = \{\hat{p}_i\}$, $i \in \mathbb{I} = \langle 0, 1, \dots, |\mathcal{P}| - 1 \rangle$, be a set of 3D pose configurations within map M , such that $f_\psi^M(\mathcal{P}) = \Psi$. Let \mathbb{I}^* be the set of indices such that $\Psi[\mathbb{I}^*] = \Psi_\uparrow$. A τ -field on map M $f_\tau^M : \mathbb{R}^2 \times [-\pi, +\pi) \rightarrow \mathbb{Z}_{\geq 0}$ is a mapping of 3D pose configurations \mathcal{P} to non-negative integers such that if $f_\psi^M(\mathcal{P}) = f_\psi^M(\mathcal{P}[\mathbb{I}^*]) = \Psi$ then $f_\tau^M(\mathcal{P}[\mathbb{I}^*]) = \mathbb{I}$. In other words a rank field maps the elements of pose estimate set $\{\hat{p}_i\}$ to the ranks \mathbb{I}^* of their corresponding CAER values in hierarchy Ψ_\uparrow .

Definition VI. Field densities.—The locational and angular density, d_l and d_α respectively, of a ψ - or τ -field express, correspondingly, the number of pose estimates per unit area of space and per angular unit, where $d_l, d_\alpha \in \mathbb{N}$.

Definition VII. Admissibility of solution.—A pose estimate $\hat{p}(\hat{x}, \hat{y}, \hat{\theta}) \in \mathbb{R}^2 \times [-\pi, +\pi)$ may be deemed an admissible solution to Problem P iff $\|\hat{l} - \hat{l}\|_2 \leq \delta_l$ and $|\hat{\theta} - \hat{\theta}| \leq \delta_\theta$ and $\|\mathbf{p} - \hat{\mathbf{p}}\|_2 \leq \delta$, where $\delta_l, \delta_\theta, \delta \in \mathbb{R}_{>0}$: $\delta_l^2 + \delta_\theta^2 = \delta^2$.

III. RELATED WORK

IV. THE CBGL METHOD

A. Motivation

The proposed method's motivation lies in the simple but powerful fact that, in general, is exhibited through figure 1: Assume a pose estimate residing in a neighbourhood of a 2D LIDAR sensor's pose within a given map; then the CAER metric between the scan measured by the sensor and the map-scan captured from the estimate within the map—the CAER metric is simultaneously proportional to both the estimate's location error and orientation error. Formally the proposed method's foundations rest on Observation O:

Observation O. It may be observed that there are conditions such that Hypothesis H stands true.

Hypothesis H. There exists $\hat{p} \in \mathbb{R}^2 \times [-\pi, +\pi)$ such that $\hat{p} \in \mathcal{V} : \|\mathbf{p} - \hat{\mathbf{p}}\|_2 \leq \delta \leq \delta_0$ is an admissible pose estimate solution to Problem P (def. VII), where set \mathcal{V} and δ_0 are defined by Conjecture C.

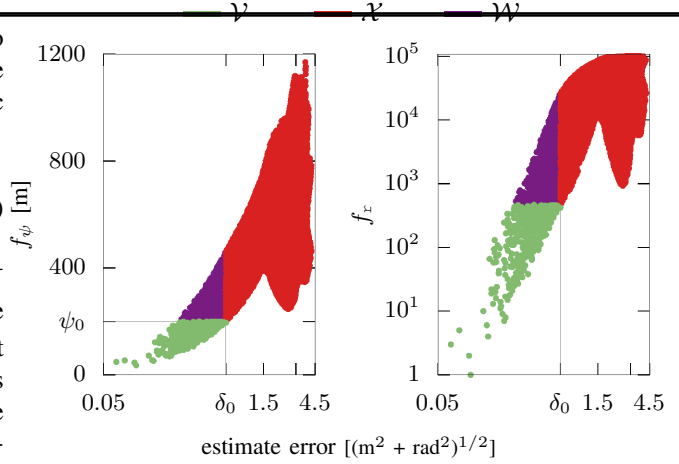


Fig. 2: The ψ -field (left) and τ -field (right) of a configuration where Observation O can be made for $\delta \leq \delta_0$

Conjecture C. Let the unknown pose of a 2D range sensor measuring range scan \mathcal{S}_R (def. I) be $\mathbf{p}(x, y, \theta)$ with respect to the reference frame of map M . Let \mathcal{H} be a set of pose hypotheses within the free (i.e. traversable) space of M : $\mathcal{H} = \{\hat{p}_i(\hat{x}_i, \hat{y}_i, \hat{\theta}_i)\} \subseteq \text{free}(M)$, $i \in \mathbb{I} = \langle 0, 1, \dots, |\mathcal{H}| - 1 \rangle$. Let f_ψ^M be the ψ -field on M (def. IV) such that $f_\psi^M(\mathcal{H}) = \Psi$. Let the field's locational and orientational densities be d_l and d_α . Let $\hat{p}_\omega \in \mathcal{H}$ and $\psi_0, \delta_0 \in \mathbb{R}_{>0}$ such that $f_\psi^M(\hat{p}_\omega) = \psi_0$ and $\|\mathbf{p} - \hat{\mathbf{p}}_j\|_2 \leq \delta_0$ for all $\hat{p}_j \in \mathcal{H} : f_\psi^M(\hat{p}_j) \leq \psi_0$. Let now $\mathcal{V} = \{\hat{p}_i \in \mathcal{H} : f_\psi^M(\hat{p}_i) \leq \psi_0, \|\mathbf{p} - \hat{\mathbf{p}}_i\|_2 \leq \delta_0\}$. Without loss of generality there exist d_l, d_α , and ψ_0, δ_0 such that for all $\hat{p}_\nu \in \mathcal{V}$:

$$f_\psi^M(\hat{p}_\nu) < f_\psi^M(\hat{p}) \Leftrightarrow \|\mathbf{p} - \hat{\mathbf{p}}_\nu\|_2 < \|\mathbf{p} - \hat{\mathbf{p}}\|_2$$

for any $\hat{p} \in \mathcal{X} = \mathcal{H} \setminus \mathcal{V} : \|\mathbf{p} - \hat{\mathbf{p}}\|_2 > \delta_0$.

Remark I. The composition of $\mathcal{H} = \mathcal{V} \cup \mathcal{X} \cup \mathcal{W}$, where $\mathcal{W} = \hat{p} \in \mathcal{H} \setminus \mathcal{V} : \|\mathbf{p} - \hat{\mathbf{p}}\|_2 \leq \delta_0$. With regard to the elements of set \mathcal{W} : if a global localisation system's output was pose $\hat{p}_\mathcal{W} \in \mathcal{W}$ then, in the language of classification, $\hat{p}_\mathcal{W}$ would constitute a false negative: it may be that $f_\psi^M(\hat{p}_\mathcal{W}) > f_\psi^M(\hat{p}_\mathcal{X})$ but with regard to the pose error: $\|\mathbf{p} - \hat{\mathbf{p}}_\mathcal{X}\|_2 \leq \delta_0$ and $\|\mathbf{p} - \hat{\mathbf{p}}_\mathcal{W}\|_2 \leq \delta_0$.

In simple terms Conjecture C states that, in general, given a dense enough set of pose hypotheses \mathcal{H} over a map M , it is possible to partition \mathcal{H} into (non-empty) sets \mathcal{V} , \mathcal{X} , and \mathcal{W} such that the error of pose estimates in set \mathcal{V} and their corresponding CAER values are simultaneously lower than those of estimates in set \mathcal{X} . Hypothesis H restrictingly states that \mathcal{V} is populated by a pose estimate whose error is such that it is deemed an admissible solution to Problem P.

B. The CBGL System

In the same vein as Hypothesis H assume the τ -field $f_\tau^M(\mathcal{H})$ corresponding to the ψ -field $f_\psi^M(\mathcal{H})$ on a given map M (def. V) such that $\Psi[\mathbb{I}^*] = \Psi_\uparrow$, and $f_\tau^M(\mathcal{H}[\mathbb{I}^*]) = \mathbb{I}$. Then the top $k \ll |\mathcal{H}|$ ranked pose hypotheses $\mathcal{H}[\mathbb{I}^*]_{0:k-1}$

Algorithm III: sm2

Input: $\mathcal{S}_R, \mathbf{M}, \hat{\mathbf{p}}$

Output: $\hat{\mathbf{p}}'$

- 1: $\mathcal{S}_V \leftarrow \text{scan_map}(\mathbf{M}, \hat{\mathbf{p}})$
 - 2: $\Delta \mathbf{p} \leftarrow \text{scan-match}(\mathcal{S}_R, \mathcal{S}_V)$ (e.g. ICP [4], FSM [5])
 - 3: $\hat{\mathbf{p}}' \leftarrow \hat{\mathbf{p}} + \Delta \mathbf{p}$
 - 4: **return** $\hat{\mathbf{p}}'$
-

define set \mathcal{V} such that $\psi_0 = \max_{\psi} f_{\psi}^M(\mathcal{H}[\mathbf{I}^*]_{0:k-1})$, and for all $\hat{\mathbf{p}}_{\mathcal{V}} \in \mathcal{V}$ and any $\hat{\mathbf{p}}_{\mathcal{X}} \in \mathcal{X}$: $f_{\mathbf{r}}^M(\hat{\mathbf{p}}_{\mathcal{V}}) < f_{\mathbf{r}}^M(\hat{\mathbf{p}}_{\mathcal{X}}) \Leftrightarrow f_{\psi}^M(\hat{\mathbf{p}}_{\mathcal{V}}) < f_{\psi}^M(\hat{\mathbf{p}}_{\mathcal{X}}) \Leftrightarrow \|\mathbf{p} - \hat{\mathbf{p}}_{\mathcal{V}}\|_2 < \|\mathbf{p} - \hat{\mathbf{p}}_{\mathcal{X}}\|_2$. By identifying the pose estimates that correspond to the bottom k CAER values, this rationale attempts to recover the identity of the pose hypotheses with the bottom k pose errors across \mathcal{H} . It constitutes the core of the proposed passive global localisation method, termed CBGL, and is described in block diagram form in figure 4 and in pseudocode in algorithm II.

Assuming the satisfaction of Observation O, the challenge is choosing such k , d_l , and d_{α} that, given pose estimate error requirement δ (def. VII; hyp. H), CBGL produces admissible pose estimates while being executed in timely manner. Given the rank field's Monte Carlo nature, optimistically, the only option for increasing the accuracy of the final pose estimate by a factor of two is doubling the densities of the \mathbf{r} -field; instead of doing that, and thereby doubling the method's execution time, subsequent to the estimation of the pose estimates with the k lowest CAER values, CBGL utilises scan-to-map-scan matching [2], [3], followed by the estimation of the one pose estimate with the lowest CAER value within the group of matched estimates.

Matching allows for (a) the correction of the pose of true positive estimates by scan-matching the map-scan captured within the map from the pose of a pose estimate against the range scan measured by the real sensor, (b) by the same token the potential divergence of spurious, false positive, pose estimates, and hence their elimination as pose estimate candidates, (c) the production of finer pose estimates without excessive increase in execution time, and (d) the decoupling of the final pose estimate's error from the field's density. Selecting among all matched estimates the one with the minimum (updated) CAER allows for the system's delivery of one pose estimate response. Figure 3 and algorithm I present the proposed method of CBGL in block diagram and algorithmic forms respectively.

V. EXPERIMENTAL EVALUATION

VI. CHARACTERISATION & LIMITATIONS

VII. CONCLUSION

REFERENCES

- [1] M. Cooper, J. Raquet, and R. Patton, "Range Information Characterization of the Hokuyo UST-20LX LIDAR Sensor," *Photonics*, 2018.
- [2] G. Vasiljević, D. Miklić, I. Draganjac, Z. Kovačić, and P. Lista, "High-accuracy vehicle localization for autonomous warehousing," *Robotics and Computer-Integrated Manufacturing*, 2016.

Algorithm I: CBGL

Input: $\mathcal{S}_R, \mathbf{M}, (d_l, d_{\alpha}), k$

Output: Pose estimate of sensor measuring range scan \mathcal{S}_R

- 1: $A \leftarrow \text{calculate_area}(\text{free}(\mathbf{M}))$
 - 2: $\mathcal{H} \leftarrow \{\emptyset\}$
 - 3: **for** $i \leftarrow 0, 1, \dots, d_l \cdot A - 1$ **do**
 - 4: $(\hat{x}, \hat{y}, \hat{\theta}) \leftarrow \text{rand}(): (x, y) \in \text{free}(\mathbf{M}), \hat{\theta} \in [-\pi, +\pi]$
 - 5: **for** $j \leftarrow 0, 1, \dots, d_{\alpha} - 1$ **do**
 - 6: $\mathcal{H} \leftarrow \{\mathcal{H}, (\hat{x}, \hat{y}, \hat{\theta} + j \cdot 2\pi/d_{\alpha})\}$
 - 7: **end for**
 - 8: **end for**
 - 9: $\mathcal{H}_1 \leftarrow \text{bottom_k_poses}(\mathcal{S}_R, \mathbf{M}, \mathcal{H}, k)$ (Alg. II)
 - 10: $\mathcal{H}_2 \leftarrow \{\emptyset\}$
 - 11: **for** $k \leftarrow 0, 1, \dots, |\mathcal{H}_1| - 1$ **do**
 - 12: $\hat{\mathbf{h}}' \leftarrow \text{sm2}(\mathcal{S}_R, \mathbf{M}, \mathcal{H}_1[k])$ (Alg. III or e.g. x1 [3])
 - 13: $\mathcal{H}_2 \leftarrow \{\mathcal{H}_2, \hat{\mathbf{h}}'\}$
 - 14: **end for**
 - 15: **return** $\text{bottom_k_poses}(\mathcal{S}_R, \mathbf{M}, \mathcal{H}_2, 1)$
-

Algorithm II: bottom_k_poses

Input: $\mathcal{S}_R, \mathbf{M}, \mathcal{H}, k$

Output: \mathcal{H}_{∇}

- 1: $\Psi \leftarrow \{\emptyset\}$
 - 2: **for** $h \leftarrow 0, 1, \dots, |\mathcal{H}| - 1$ **do**
 - 3: $\mathcal{S}_V^h \leftarrow \text{scan_map}(\mathbf{M}, \mathcal{H}[h])$
 - 4: $\psi \leftarrow 0$
 - 5: **for** $n \leftarrow 0, 1, \dots, |\mathcal{S}_R| - 1$ **do**
 - 6: $\psi \leftarrow \psi + |\mathcal{S}_R[n] - \mathcal{S}_V^h[n]|$ (Eq. (1))
 - 7: **end for**
 - 8: $\Psi \leftarrow \{\Psi, \psi\}$
 - 9: **end for**
 - 10: $[\Psi_{\uparrow}, \mathbf{I}^*] \leftarrow \text{sort}(\Psi, \text{asc})$
 - 11: $\mathcal{H}_{\nabla} \leftarrow \{\emptyset\}$
 - 12: **for** $h \leftarrow 0, 1, \dots, k - 1$ **do**
 - 13: $\mathcal{H}_{\nabla} \leftarrow \{\mathcal{H}_{\nabla}, \mathcal{H}[\mathbf{I}^*[h]]\}$
 - 14: **end for**
 - 15: **return** \mathcal{H}_{∇}
-

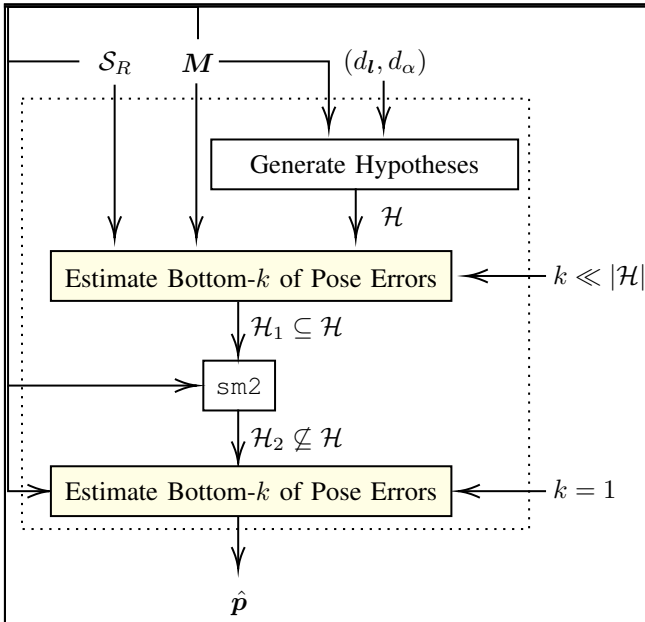


Fig. 3: CBGL in block diagram form. Given a LIDAR's 2D measurement \mathcal{S}_R and the map \mathcal{M} that represents the environment in which the sensor is posed, CBGL generates a set of pose hypotheses \mathcal{H} and invokes the estimation of the k hypotheses with the least pose error (fig. 4; alg. II). Then it scan-to-map-scan matches those to the measurement for finer estimation and outlier rejection (alg. III). CBGL's output pose estimate is that with the least CAER among matched estimates

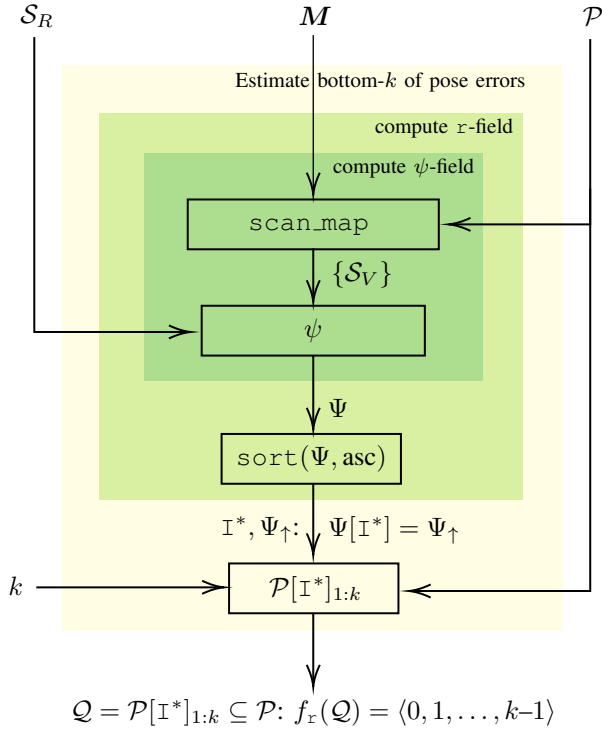


Fig. 4: CBGL's core method. Given a LIDAR's 2D measurement \mathcal{S}_R , the map \mathcal{M} that represents the environment in which the sensor is posed, and a set of pose hypotheses \mathcal{H} , CBGL (a) computes and ranks the CAER values between the measurement and map-scans captured from the hypotheses within the map, and (b) outputs the hypotheses with the k lowest CAER values

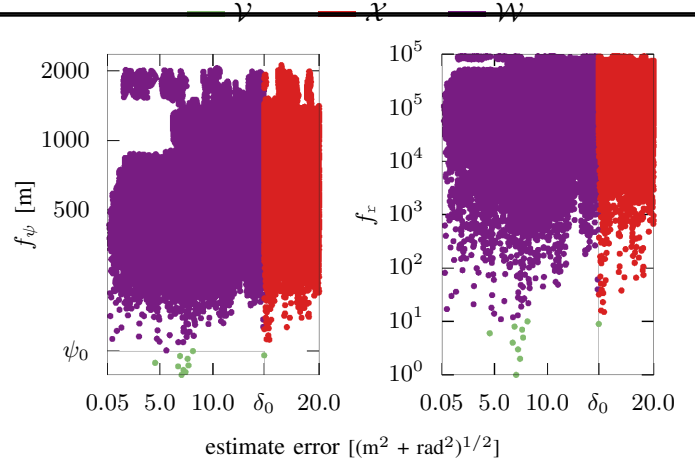


Fig. 5: Contrary to fig. 2: the ψ -field (left) and r -field (right) of a configuration where Observation O cannot be made: set \mathcal{V} is empty of admissible pose estimates for $\delta < 4.5 (\text{m}^2 + \text{rad}^2)^{1/2}$. The effect is in fact produced due to the repetition of the immediate environment of the sensor more than once in the given map and its apparent dissimilarity to its corresponding portion of the map

[3] A. Filotheou, A. L. Symeonidis, G. D. Sergiadis, and A. G. Dimitriou, "Correspondenceless scan-to-map-scan matching of 2D panoramic range scans," *Array*, 2023.

[4] I. Vizzo, T. Guadagnino, B. Mersch, L. Wiesmann, J. Behley, and C. Stachniss, "KISS-ICP: In Defense of Point-to-Point ICP Simple, Accurate, and Robust Registration If Done the Right Way," *IEEE Robotics and Automation Letters*, 2023.

[5] A. Filotheou, G. D. Sergiadis, and A. G. Dimitriou, "FSM: Correspondenceless scan-matching of panoramic 2D range scans," in *2022 IEEE/RSJ International Conference on Intelligent Robots and Systems (IROS)*. IEEE, 2022.